 CMES, vol.45, no.1, pp.1-29, 2009

A Galerkin Boundary Node Method for Two-Dimensional Linear Elasticity

Xiaolin Li[1] **and Jialin Zhu**[2]

Abstract: In this paper, a Galerkin boundary node method (GBNM) is developed for boundary-only analysis of 2D problems in linear elasticity. The GBNM combines the variational form of a boundary integral formulation for the elastic equations with the moving least-squares approximations for generating the trial and test functions. Unlike the boundary node method, the main idea here is to use the Galerkin scheme for numerical analysis, thus boundary conditions in the GBNM can be satisfied easily and directly in the weak formulation of the boundary integral equation. Another advantage with the Galerkin scheme is that the GBNM can keep the symmetry and positive definiteness of the variational problems. The error analysis and convergence study of the GBNM in Sobolev spaces are given. Numerical examples are also presented to show the efficiency of the method.

Keywords: Meshless, moving least-squares, boundary integral equations, Galerkin boundary node method.

1 Introduction

Boundary integral equations (BIEs) have widely used for the solution of a variety of boundary value problems in potential theory and classical elasticity. The numerical discretization of BIEs is commonly known as the boundary element method (BEM) [Dautray and Lious (2000); Hsiao and Wendland (2008); Zhu and Yuan (2009)]. The BEM is a well developed and powerful numerical method for linear and exterior problems as it can reduce the dimensionality of the original problem by one. However, the BEM still requires boundary discretization, which may cause some inconvenience in the implementation, such as attacking complicated boundary problems and moving boundary problems.

In attempts to reduce the meshing-related difficulties, a new type of method called

[1] Corresponding author. College of Mathematics and Computer Science, Chongqing Normal University, Chongqing 400047, P R China. E-mail: lxlmath@163.com.
[2] College of Mathematics and Physics, Chongqing University, Chongqing 400044, P R China.

meshless or meshfree method has been developed in recent years. The main feature of this type of method is the absence of an explicit mesh, and the approximate solution is constructed entirely based on a set of scattered nodes. Different kinds of meshless methods, such as the smoothed particle hydrodynamics [Moulinec, Issa, Marongiu, and Violeau (2008)], the element free Galerkin method (EFGM) [Belytschko, Krongauz, Organ, and Fleming (1996); Chen, Chi, and Lee (2009)], the meshless local Petrov-Galerkin (MLPG) method [Atluri and Shen (2002)], the reproducing kernel particle method [Shaw and Roy (2007); Namdeo and Manohar (2008)], the radial basis functions method [Libre, Emdadi, Kansa, Rahimian, and Shekarchi (2008)] and the h-p meshless method [Duarte and Oden (1996)] have been proposed and achieved remarkable progress in solving a wide range of boundary value problems in solid [Hagihara, Tsunori, Ikeda, and Miyazaki (2007); Wen and Hon (2007); Wu, Chiu, and Wang (2008)], fluid [Mai-Duy, Mai-Cao, and Tran-Cong (2007); Kosec and Sarler (2008); Ho-Minh, Mai-Duy, and Tran-Cong (2009)], electromagnetic [Shim, Ho, Wang, and Tortorelli (2008); Haq, Islam, and Ali (2008)] and dynamic [Liu, Chen, Li, and Cen (2008); Haq, Islam, and Uddin (2009)]. Particularly, these methods has also been successfully applied for problems with moving interface [Mai-Cao and Tran-Cong (2008)], large deformation [Wong and Shie (2008); Chen, Chi, and Lee (2009)] and crack propagation [Wen, Aliabadi, and Liu (2008); Zhang and Chen (2008); Sageresan and Drathi (2008); Li, Liu, and Wang (2008)]. These meshless methods followed the idea as the finite element method (FEM), in which the problem domain is discretized.

The idea of meshless has also been applied in BIEs, such as the boundary node method (BNM) [Mukherjee and Mukherjee (1997)], the meshless local boundary integral equation (LBIE) method [Atluri, Sladek, Sladek, and Zhu (2000)] and the boundary point interpolation method (BPIM) [Gu and Liu (2002). In these BIEs-based methods, the LBIE method is equivalent to a sort of MLPG approaches, which use local weak forms over a local sub-domain and shape functions from the moving least-squares (MLS) approximations. The LBIE method and the MLPG methods are very promising methods, and have been implemented for problems in potential theory [Pini, Mazzia, and Sartoretto (2008)], elasticity [Atluri, Sladek, Sladek, and Zhu (2000); Han and Atluri (2004); Atluri, Liu, and Han (2006); Long, Liu, and Li (2008); Sellountos, Sequeira1, and Polyzos (2009); Zheng, Long, Xiong, and Li (2009); Sladek, Sladek, and Solek (2009)], heat conduction [Wu, Shen, and Tao (2007); Sladek, Sladek, Tan, and Atluri (2008)], thermodynamics [Sladek, Sladek, Zhang, and Solek (2007); Sladek, Sladek, Solek, and Wen (2008); Sladek, Sladek, Solek, Wen, and Atluri (2008)], magnetics [Johnson and Owen (2007); Zhao and Nie (2008)] and fluid [Ma (2007); Arefmanesh, Najafi, and Abdi (2008); Mohammadi (2008); Ma and Zhou (2009)]. The LBIE method, however, is

not strictly a boundary method since it requires evaluation of integrals over certain surfaces (called L_s in [Atluri, Sladek, Sladek, and Zhu (2000)]) that can be regarded as 'closure surfaces' of boundary elements.

The BNM is formulated using the MLS approximations and the technique of BIEs. Compared to the LBIE method and other domain type meshless methods, this approach and the BPIM require only a nodal data structure on the bounding surface of a body whose dimension is less than that of the domain itself. So like the BEM, they are superior in treating problems dealing with infinite or semi-infinite domains. The BNM has been successfully applied for the solution of problems in potential theory [Mukherjee and Mukherjee (1997)] and linear elasticity [Kothnur, Mukherjee, and Mukherjee (1999)]. However, because the MLS approximations lack the delta function property, it is difficulty to exactly satisfy boundary conditions in the BNM. The strategy used in the BNM to impose boundary conditions involves a new definition of the discrete norm used for the construction of the MLS approximations. This strategy doubles the number of system equations. Recently, based on using the point interpolation method to construct shape functions, Gu and Liu (2002) developed the BPIM to solve 2D elastostatics. The BPIM can exactly satisfy boundary conditions, since its shape functions possess delta function property. But the compatibility of field function approximation cannot be always ensured in this method [Liu and Gu (2004)]. In addition, as in the BNM, the system matrices in the BPIM are nonsymmetric.

A boundary-type meshless method, the Galerkin boundary node method (GBNM), is discussed in this paper. In this approach, an equivalent variational form of a BIE is used for representing the boundary value problem, and the trial and test functions of the weak formulation are constructed by the MLS approximations. An advantage with the Galerkin scheme is that boundary conditions can be satisfied easily and directly via multiplying the MLS shape function and integrating over the boundary. Besides, the GBNM inherits the symmetry and positive definiteness of the variational problems. Symmetrical formulations improve solution efficiency and can be easily coupled with the FEM or other established meshless methods such as the EFGM. This coupled technique is especially suited for problems with an unbounded domain. The GBNM has been applied to problems in potential theory [Li and Zhu (2009a,b)]. In this paper, we extend the frontiers of the GBNM for boundary-only analysis of the interior and exterior linear elastic problems in two dimensions.

It is well known that one limitation of the meshless methods found in the literature is that few of them have a rich mathematical background to justify their use. Namely, mathematical proofs of conditions sufficient to guarantee that these methods will converge to the true solution are not available. To the best of our knowl-

edge, the theoretical basis of BIEs-based meshless methods is just being studied and far from completion. In this article, we also provide error estimates for the GBNM in Sobolev spaces.

An outline of this paper is as follows. In Section 2, we introduce some notations to be used later. Section 3 presents the MLS scheme. Section 4 gives a detailed numerical implementation of the GBNM for 2D linear elasticity. The convergence of this approach will be stated in Section 5. Section 6 provides some numerical results. Section 7 contains conclusions.

2 Notations

Let Γ be a smooth, simple closed curve in the plane and let Ω and Ω' denote its interior and exterior respectively. A generic point in $\mathbb{R}^2$ is denoted by $\mathbf{x} = (x_1, x_2)$ or $\mathbf{y} = (y_1, y_2)$.

For any point $\mathbf{x} \in \Gamma$, we use $\Re(\mathbf{x})$ to denote the domain of influence of $\mathbf{x}$. Let $Q_N = \{\mathbf{x}_i\}_{i=1}^N$ be an arbitrarily chosen set of N boundary nodes $\mathbf{x}_i$. The set Q_N is used for defining a finite open covering $\{\Re_i\}_{i=1}^N$ of Γ composed of N balls $\Re_i$ centered at the points $\mathbf{x}_i$, $i = 1, 2, \cdots, N$, where $\Re_i = \Re(\mathbf{x}_i)$ is the domain of influence of $\mathbf{x}_i$.

Assume that there have $\kappa(\mathbf{x})$ boundary nodes that lie on $\Re(\mathbf{x})$. Then, we use the notation $I_1, I_2, \cdots, I_\kappa$ to express the global sequence number of these nodes, and define $\wedge(\mathbf{x}) = \{I_1, I_2, \cdots, I_\kappa\}$.

Let w_i, $i = 1, 2, \cdots, N$, denote weight functions that belong to the space $C_0^\ell(\Re_i)$, $\ell \geq 0$, with the following properties:

$$w_i(\mathbf{x}) > 0, \ \forall \mathbf{x} \in \Re_i; \quad \sum_{i \in \wedge(\mathbf{x})} w_i(\mathbf{x}) = 1, \ \forall \mathbf{x} \in \Gamma \tag{1}$$

Besides, we use the notation

$$\Re^i = \{\mathbf{x} \in \Gamma : \mathbf{x}_i \in \Re(\mathbf{x})\}, \quad 1 \leq i \leq N \tag{2}$$

for the set of boundary points whose influence domain includes the boundary node $\mathbf{x}_i$. We emphasize that for different boundary point $\mathbf{x}$, because $\Re(\mathbf{x})$ varies from point to point, $\Re^i \equiv \Re_i$ if and only if the radii of $\Re(\mathbf{x})$ is a constant for any $\mathbf{x} \in \Gamma$.

Let τ be an arbitrary real number, we denote by $H^\tau(\Gamma)$ the Sobolev spaces as well as their interpolation spaces on Γ for noninteger τ [Hsiao and Wendland (2008); Zhu and Yuan (2009)]. Moreover, we define the following weighted Sobolev space

[Dautray and Lious (2000); Hsiao and Wendland (2008); Zhu and Yuan (2009)]

$$W_0^1\left(\Omega'\right) = \left\{ v \in \mathscr{D}'\left(\Omega'\right) : \frac{v}{\sqrt{1+r^2}\ln\left(2+r^2\right)} \in L^2\left(\Omega'\right), \frac{\partial v}{\partial x_i} \in L^2\left(\Omega'\right), i = 1,2 \right\} \quad (3)$$

where $r = \sqrt{x_1^2 + x_2^2}$. It is a reflexive Banach space equipped with its natural norm:

$$\|v\|_{W_0^1(\Omega')} = \left(\left\| \frac{v}{\sqrt{1+r^2}\ln\left(2+r^2\right)} \right\|^2_{L^2(\Omega')} + \sum_{i=1}^{2} \left\| \frac{\partial v}{\partial x_i} \right\|^2_{L^2(\Omega')} \right)^{1/2} \quad (4)$$

Observe that all the local properties of the space $W_0^1\left(\Omega'\right)$ coincide with those of the Sobolev space $H^1\left(\Omega'\right)$. As a consequence, the traces of these functions on Γ satisfy the usual trace theorems.

3 The moving least squares (MLS) method

In the MLS method, the numerical approximation starts from a cluster of scattered nodes instead of elements. Assume that $\mathbf{x}(s) \in \Gamma$, the MLS approximation for a given function v is defined as [Li and Zhu (2009a)]

$$v(\mathbf{x}) \approx \mathscr{M} v(\mathbf{x}) = \sum_{i=1}^{N} \Phi_i(\mathbf{x}) v_i \quad (5)$$

where $\mathscr{M}$ is an approximation operator, and

$$\Phi_i(\mathbf{x}(s)) = \begin{cases} \sum_{j=0}^{\beta} P_j(s) \left[\mathbf{A}^{-1}(s)\mathbf{B}(s)\right]_{jk}, & i = I_k \in \wedge(\mathbf{x}) \\ 0, & i \notin \wedge(\mathbf{x}) \end{cases} \quad (6)$$

and the matrices $\mathbf{A}(s)$ and $\mathbf{B}(s)$ being defined by

$$\mathbf{A}(s) = \sum_{i \in \wedge(\mathbf{x}(s))} w_i(s) \mathbf{P}(s_i) \mathbf{P}^{\mathrm{T}}(s_i) \quad (7)$$

$$\mathbf{B}(s) = \left[w_{I_1}(s)\mathbf{P}(s_{I_1}), w_{I_2}(s)\mathbf{P}(s_{I_2}), \cdots, w_{I_\kappa}(s)\mathbf{P}(s_{I_\kappa}) \right] \quad (8)$$

in which s is a local co-ordinate of the boundary point $\mathbf{x}$ on Γ, $\mathbf{P}(s)$ is a vector of the polynomial basis, $\beta+1$ is the number of terms of the monomials.

In order to make sense of the definition of the MLS approximations, the matrix $\mathbf{A}(s)$ must be invertible. The corresponding work can be found in [Duarte and Oden (1996)].

For our subsequent error analysis the following conditions will be assumed from now on.

Assumption. There exist

- **A1.** A nonnegative integer γ such that the MLS shape functions $\Phi_i(\mathbf{x}) \in C^\gamma(\Gamma)$ and the boundary Γ is a C^γ curve.
- **A2.** An upper bound of the radii of weight functions. That is, a constant h such that the radii of weight functions is less than h.
- **A3.** A constant integer K such that each point on Γ is covered by at most K shape functions.
- **A4.** A uniform bound of the weight function and its derivatives. Namely, constants C_{w1} and C_{w2} independent with h such that $C_{w1}h^{-j} \leq \left\|\partial^j w_i(\mathbf{x})\right\|_{L^\infty(\Gamma)} \leq C_{w2}h^{-j}$, $1 \leq i \leq N$.

Remark 3.1 *From [Duarte and Oden (1996)], if monomials P_j ($j = 0,1,\cdots,\beta$) and weight functions w_i ($i = 1,2,\cdots,N$) are γ-times continuously differentiable, then $\Phi_i(\mathbf{x}) \in C^\gamma(\Gamma)$.*

Remark 3.2 *Assumption (A3) is quite natural since, otherwise, as the number of boundary nodes lie on a local area increases, the shape functions tend to be more and more linearly dependent in the local area.*

We list below some properties of the MLS shape functions Φ_i [Li and Zhu (2009a)].

Property 3.1 $\Phi_i(\mathbf{x}) \in C_0^\gamma\left(\Re^i\right)$, $1 \leq i \leq N$.

Property 3.2 *We have a constant C independent of h such that*

$$\left\|\Phi_i(\mathbf{x})\right\|_{H^k(\Gamma)} \leq Ch^{m-k}\left\|\Phi_i(\mathbf{x})\right\|_{H^m(\Gamma)}, \quad 1 \leq i \leq N,\ -\gamma \leq m \leq k,\ 0 \leq k \leq \gamma \tag{9}$$

The following theorem gives an approximation estimate for the MLS scheme, which is central to the convergence proof of the proposed GBNM [Li and Zhu (2009a)].

Theorem 3.1 *Assume that $v(\mathbf{x}) \in H^{\gamma+1}(\Gamma)$. Let $\mathscr{M}v(\mathbf{x}) = \sum_{i=1}^N \Phi_i(\mathbf{x})v_i$, then*

$$\left\|v(\mathbf{x}) - \mathscr{M}v(\mathbf{x})\right\|_{H^k(\Gamma)} \leq Ch^{\gamma+1-k}\left\|v(\mathbf{x})\right\|_{H^{\gamma+1}(\Gamma)} \tag{10}$$

where $0 \leq k \leq \gamma$ and C is a constant independent of h.

4 The Galerkin boundary node method

In this section the GBNM for the approximation of 2D linear elasticity is introduced. In this approach, meshless shape functions are constructed with the MLS technique and are used in a Galerkin setting for the approximation of the weak form of BIEs.

4.1 Galerkin procedures

We consider the boundary value problem consisting of the linear elastic equation for the displacement field $\mathbf{u} = (u_1, u_2)$:

$$\begin{cases} \mu\Delta\mathbf{u} + (\lambda+\mu)\,\mathrm{grad}\,(\mathrm{div}\,\mathbf{u}) = 0, & \text{in } \Omega \text{ or } \Omega' \\ \mathbf{u}|_\Gamma = \mathbf{g}, & \text{on } \Gamma \end{cases} \tag{11}$$

where $\mu > 0$ and $\lambda > -\mu$ are given Lamé constants, and $\mathbf{g} = (g_1, g_2)$ is a prescribed function on Γ. In the case of the exterior problem, we append to problem (11) the following condition at infinity:

$$|u_i(\mathbf{x})| = O(1), \quad i = 1,2, \quad \text{as } |\mathbf{x}| \to \infty \tag{12}$$

We introduce the stress tensor σ and strain tensor ε

$$\sigma_{ij}(\mathbf{u}) = \lambda\delta_{ij}\sum_{k=1}^{2}\varepsilon_{kk}(\mathbf{u}) + 2\mu\varepsilon_{ij}(\mathbf{u});\ \varepsilon_{ij}(\mathbf{u}) = \frac{1}{2}\left(\frac{\partial u_i}{\partial x_j} + \frac{\partial u_j}{\partial x_i}\right), \quad i,j = 1,2 \tag{13}$$

where δ_{ij} is the Kronecker symbol. Let $\mathbf{q} = (q_1, q_2)$ stands for the jump through Γ of $\mathbf{n}\cdot\sigma(\mathbf{u})$, i.e.,

$$q_i = \sum_{j=1}^{2}\sigma_{ij}(\mathbf{u})\,n_j\Big|_\Gamma^{\text{int}} - \sum_{j=1}^{2}\sigma_{ij}(\mathbf{u})\,n_j\Big|_\Gamma^{\text{ext}}, \quad i = 1,2 \tag{14}$$

where $\mathbf{n}$ is the outward normal direction on Γ. Then as indicated in [Hsiao and Wendland (2008); Zhu and Yuan (2009)], condition (12) implies that

$$\int_\Gamma q_i(\mathbf{y})\,\mathrm{d}S_\mathbf{y} = 0, \quad i = 1,2 \tag{15}$$

The classical way of solving problem (11) using integral equations consists in using a simple layer representation. Let U_{ij}^* $(i,j = 1,2)$ be the Kelvin solution

$$U_{ij}^*(\mathbf{x},\mathbf{y}) = \frac{\lambda+3\mu}{4\pi\mu(\lambda+2\mu)}\left[\delta_{ij}\ln\frac{1}{r} + \frac{\lambda+\mu}{(\lambda+3\mu)}r_{,i}r_{,j}\right] \tag{16}$$

where $r = |\mathbf{x}-\mathbf{y}|$ and $r_{,i} = (x_i - y_i)/r$. Then the solution of the elastic problem (11) can be represented as

$$u_j(\mathbf{x}) = \sum_{i=1}^{2} \int_\Gamma U_{ij}^*(\mathbf{x},\mathbf{y})\, q_i(\mathbf{y})\, \mathrm{d}S_\mathbf{y} + \xi_j, \quad \mathbf{x} \in \mathbb{R}^2 \tag{17}$$

in which $\xi = (\xi_1, \xi_2)$ is an unknown constant vector. The unknown ξ arises because the displacement field at infinity is not zero for 2D problems.

From Eqs. (13) and (17), the stress σ reads

$$\sigma_{ij}(\mathbf{x}) = \sum_{k=1}^{2} \int_\Gamma D_{kij}^*(\mathbf{x},\mathbf{y})\, q_k(\mathbf{y})\, \mathrm{d}S_\mathbf{y}, \quad \mathbf{x} \in \mathbb{R}^2 \tag{18}$$

where the third order tensor component $D_{kij}^*\ (k,i,j=1,2)$ is

$$\begin{aligned} D_{kij}^*(\mathbf{x},\mathbf{y}) &= \lambda\delta_{ij} \sum_{l=1}^{2} \frac{\partial U_{kl}^*}{\partial x_l} + \mu\left(\frac{\partial U_{ki}^*}{\partial x_j} + \frac{\partial U_{kj}^*}{\partial x_i}\right) \\ &= \frac{-1}{2\pi(\lambda+2\mu)\, r}\left[\mu\left(\delta_{ki}r_{,j} + \delta_{kj}r_{,i} - \delta_{ij}r_{,k}\right) + 2(\lambda+\mu)\, r_{,i}r_{,j}r_{,k}\right] \end{aligned} \tag{19}$$

Now giving $\mathbf{g} \in \left(H^{1/2}(\Gamma)\right)^2$, Eq. (17) leads to the boundary relation

$$g_j(\mathbf{x}) = \sum_{i=1}^{2} \int_\Gamma U_{ij}^*(\mathbf{x},\mathbf{y})\, q_i(\mathbf{y})\, \mathrm{d}S_\mathbf{y} + \xi_j, \quad \mathbf{x} \in \Gamma \tag{20}$$

which is suitable for the solution of the interior as well as the exterior problem.

Let

$$\overset{\circ}{H}{}^k(\Gamma) = \left\{ f \in H^k(\Gamma), \int_\Gamma f(\mathbf{y})\, \mathrm{d}S_\mathbf{y} = 0 \right\}, \quad k \in \mathbb{R} \tag{21}$$

then formula (20) is associated with the following variational problem: find $\mathbf{q} \in \left(\overset{\circ}{H}{}^{-1/2}(\Gamma)\right)^2$ such that

$$b(\mathbf{q},\mathbf{q}') = \sum_{j=1}^{2} \int_\Gamma g_j(\mathbf{x})\, q_j'(\mathbf{x})\, \mathrm{d}S_\mathbf{x}, \quad \forall \mathbf{q}' \in \left(\overset{\circ}{H}{}^{-1/2}(\Gamma)\right)^2 \tag{22}$$

with

$$b(\mathbf{q},\mathbf{q}') = \sum_{i,j=1}^{2} \int_\Gamma \int_\Gamma U_{ij}^*(\mathbf{x},\mathbf{y})\, q_i(\mathbf{y})\, q_j'(\mathbf{x})\, \mathrm{d}S_\mathbf{y}\, \mathrm{d}S_\mathbf{x} \tag{23}$$

As in the three dimensional case [Dautray and Lious (2000); Zhu and Yuan (2009)], it can be verified that the boundary integral formulation (20) defines an isomorphism from $\overset{\circ}{H}{}^{-1/2}(\Gamma)$ onto $H^{1/2}(\Gamma)/\mathbb{R}$, and the bilinear form $b(\cdot,\cdot)$ is continuous and coercive on $\left(\overset{\circ}{H}{}^{-1/2}(\Gamma)\right)^2$ [Hsiao and Wendland (2008)]. Thus, by the Lax-Milgram theorem, we have:

Theorem 4.1 *If* $\mathbf{g} \in \left(H^{1/2}(\Gamma)\right)^2$, *then the variational prolem (22) admits a unique solution* $\mathbf{q} \in \left(\overset{\circ}{H}{}^{-1/2}(\Gamma)\right)^2$, *and the elastic problem (11) has one and only one solution* $\mathbf{u} \in \left(H^1(\Omega)\right)^2 \cup \left(W_0^1(\Omega')\right)^2$.

4.2 Approximation

Let

$$W = \operatorname{span}\{\Phi_i, 1 \le i \le N\}, \quad V_h(\Gamma) = W \times W \tag{24}$$

the basis functions Φ_i defined in Eq. (6). Let

$$\overset{\circ}{V}_h(\Gamma) = \left\{ \mathbf{f} \in V_h(\Gamma), \int_\Gamma f_i(\mathbf{y})\, \mathrm{d}S_\mathbf{y} = 0, i = 1,2 \right\} \tag{25}$$

Since Assumption (A1) implies that $\Phi_i(\mathbf{x}) \in H^m(\Gamma) \subset H^{-1/2}(\Gamma)$ for $-1/2 \le m \le \gamma$, the variational problem (22) can be approximated by: find $\mathbf{q}^h = \left(q_1^h, q_2^h\right) \in \overset{\circ}{V}_h(\Gamma)$ such that

$$b\left(\mathbf{q}^h, \mathbf{q}'\right) = \sum_{i=1}^{2} \int_\Gamma g_i(\mathbf{x})\, q_i'(\mathbf{x})\, \mathrm{d}S_\mathbf{x}, \quad \forall \mathbf{q}' \in \overset{\circ}{V}_h(\Gamma) \tag{26}$$

In this way, we must take into account the constraint

$$\int_\Gamma q_i^h(\mathbf{y})\, \mathrm{d}S_\mathbf{y} = 0, \quad i = 1,2 \tag{27}$$

in the process of approximation. For the convenience of numerical implementation we introduce a Lagrangian multiplier to replace the constraint (27). Let

$$a(\xi, \mathbf{q}) = \sum_{i=1}^{2} \int_\Gamma \xi_i q_i(\mathbf{y})\, \mathrm{d}S_\mathbf{y}, \quad \forall \mathbf{q} \in V_h(\Gamma), \quad \xi \in \mathbb{R}^2 \tag{28}$$

then the Galerkin form for problem (11) can be set as the following saddle-point problem:

$$\begin{cases} \text{find } \left(\mathbf{q}^h, \xi\right) \in V_h(\Gamma) \times \mathbb{R}^2 \text{ such that } \forall \left(\mathbf{q}', \xi'\right) \in V_h(\Gamma) \times \mathbb{R}^2 \\ b\left(\mathbf{q}^h, \mathbf{q}'\right) + a\left(\xi, \mathbf{q}'\right) = \sum_{i=1}^{2} \int_\Gamma g_i(\mathbf{x}) q_i'(\mathbf{x}) \, \mathrm{d}S_\mathbf{x} \\ a\left(\xi', \mathbf{q}^h\right) = 0 \end{cases} \tag{29}$$

The general results of [Brezzi (1974)] can be applied to the particular case, we have:

Theorem 4.2 *Problem (26) admits only one solution* $\mathbf{q}^h \in \overset{\circ}{V}_h(\Gamma)$ *and there exists* $\xi \in \mathbb{R}^2$ *such that* $\left(\mathbf{q}^h, \xi\right)$ *is the unique solution of problem (29).*

On $V_h(\Gamma)$, the Galerkin approximation $\mathbf{q}^h$ of the real solution $\mathbf{q}$ may be written as

$$q_k^h(\mathbf{x}) = \sum_{i=1}^{N} \Phi_i(\mathbf{x}) q_k^{(i)}, \quad k = 1, 2 \tag{30}$$

Substituting Eq. (30) into Eq. (29), by virtue of Property 3.1, one gets a $(2N+2) * (2N+2)$ linear system

$$\begin{Bmatrix} \begin{bmatrix} a_{ji}^{11} \\ a_{ji}^{21} \end{bmatrix} & \begin{bmatrix} a_{ji}^{12} \\ a_{ji}^{22} \end{bmatrix} & \begin{bmatrix} c_{jk}^1 \\ c_{jk}^2 \end{bmatrix} \\ \begin{bmatrix} b_{ki}^1 \end{bmatrix} & \begin{bmatrix} b_{ki}^2 \end{bmatrix} & [0] \end{Bmatrix} \begin{Bmatrix} \begin{Bmatrix} q_1^{(i)} \\ q_2^{(i)} \end{Bmatrix} \\ \{\xi_k\} \end{Bmatrix} = \begin{Bmatrix} \begin{Bmatrix} f_j^1 \\ f_j^2 \end{Bmatrix} \\ \{0\} \end{Bmatrix} \tag{31}$$

in which $i, j = 1, 2, \cdots, N$; $k = 1, 2$ and

$$a_{ji}^{ml} = \int_{\Re^j} \int_{\Re^i} U_{ml}^*(\mathbf{x}, \mathbf{y}) \Phi_i(\mathbf{y}) \Phi_j(\mathbf{x}) \, \mathrm{d}S_\mathbf{y} \, \mathrm{d}S_\mathbf{x} \tag{32}$$

$$c_{j1}^1 = b_{1j}^1 = c_{j2}^2 = b_{2j}^2 = \int_{\Re^j} \Phi_j(\mathbf{x}) \, \mathrm{d}S_\mathbf{x} \tag{33}$$

$$c_{j2}^1 = b_{2j}^1 = c_{j1}^2 = b_{1j}^2 = 0 \tag{34}$$

$$f_j^m = \int_{\Re^j} g_m(\mathbf{x}) \Phi_j(\mathbf{x}) \, \mathrm{d}S_\mathbf{x} \tag{35}$$

with $m, l = 1, 2$. Besides, $\Re^j$ and $\Re^i$ are defined by Eq. (2), and are parts of the boundary Γ. As in the EFGM and the BNM, these integrations can be numerically calculated by employing a cell structure.

Remark 4.1 *Since the cell can be of any shape and the only restriction is that the unions of all cells equal the integral area, the concept of cell is quite different from that of an element in the BEM. Thus, the GBNM is a boundary type meshless method.*

Remark 4.2 *The boundary function* $\mathbf{g}(\mathbf{x})$ *are multiplied by* $\Phi_j(\mathbf{x})$ *and integrated on* Γ. *As a consequence, boundary conditions can be implemented accurately despite the MLS approximations lacking the delta function property.*

Remark 4.3 *The system matrix in Eq. (31) is symmetric.*

Once $q_k^{(i)}$ and ξ_k are found the approximate solution $\mathbf{u}^h = \left(u_1^h, u_2^h\right)$ of displacement $\mathbf{u}$ can be evaluated from an approximation form of Eq. (17)

$$\begin{aligned} u_j^h(\mathbf{x}) &= \sum_{i=1}^{2} \int_\Gamma U_{ij}^*(\mathbf{x},\mathbf{y})\, q_i^h(\mathbf{y})\, \mathrm{d}S_\mathbf{y} + \xi_j \\ &= \sum_{i=1}^{2} \sum_{m=1}^{N} q_i^{(m)} \int_{\Re^m} U_{ij}^*(\mathbf{x},\mathbf{y})\, \Phi_m(\mathbf{y})\, \mathrm{d}S_\mathbf{y} + \xi_j, \quad j = 1,2, \quad \mathbf{x} \in \mathbb{R}^2 \end{aligned} \tag{36}$$

and the approximate solution σ^h of the stress tensor σ can be determined by

$$\begin{aligned} \sigma_{ij}^h(\mathbf{x}) &= \sum_{k=1}^{2} \int_\Gamma D_{kij}^*(\mathbf{x},\mathbf{y})\, q_k^h(\mathbf{y})\, \mathrm{d}S_\mathbf{y} \\ &= \sum_{k=1}^{2} \sum_{m=1}^{N} q_k^{(m)} \int_{\Re^m} D_{kij}^*(\mathbf{x},\mathbf{y})\, \Phi_m(\mathbf{y})\, \mathrm{d}S_\mathbf{y} + \xi_j, \quad i,j = 1,2, \quad \mathbf{x} \in \mathbb{R}^2 \end{aligned} \tag{37}$$

5 Error estimates

In this section, we will prove that the result obtained using the GBNM converge to the solution of the elastic problem (11) gradually. In order to prove some theorems, we need the following inverse property.

Lemma 5.1 *For any* $\mathbf{q}^h(\mathbf{x}) \in V_h(\Gamma)$, *there is a constant C independent of h such that*

$$\left\|\mathbf{q}^h(\mathbf{x})\right\|_{\left(H^k(\Gamma)\right)^2} \le Ch^{m-k} \left\|\mathbf{q}^h(\mathbf{x})\right\|_{(H^m(\Gamma))^2}, \quad -\gamma \le m \le k, \quad 0 \le k \le \gamma \tag{38}$$

Proof. The proof follows from Property 3.2 and involves only algebraic manipulations. Details can be found in [Li and Zhu (2009a)].

For the meshless solution $\mathbf{q}^h$ of the variational problem (26), we have the following error estimates.

Theorem 5.1 *Let* $\mathbf{q}$ *and* $\mathbf{q}^h$ *be solutions of variational problems (22) and (26), respectively. Assume that* $\mathbf{q} \in \left(H^{m+1}(\Gamma)\right)^2$*, then*

$$\left\|\mathbf{q}-\mathbf{q}^h\right\|_{\left(H^{-1/2}(\Gamma)\right)^2} \leq Ch^{m+3/2}\left\|\mathbf{q}\right\|_{(H^{m+1}(\Gamma))^2} \tag{39}$$

where $0 \leq m \leq \gamma$ *and* C *is a constant independent of* h*.*

Proof. Subtraction Eq. (26) from Eq. (22) yields

$$b\left(\mathbf{q}-\mathbf{q}^h,\mathbf{q}'\right)=0, \quad \forall \mathbf{q}' \in \overset{\circ}{V}_h(\Gamma) \tag{40}$$

then according to $\mathbf{q}'-\mathbf{q}^h \in \overset{\circ}{V}_h(\Gamma)$, and using the continuity of the bilinear form $b(\cdot,\cdot)$, one gets

$$\begin{aligned} b\left(\mathbf{q}-\mathbf{q}^h,\mathbf{q}-\mathbf{q}^h\right) &= b\left(\mathbf{q}-\mathbf{q}^h,\mathbf{q}-\mathbf{q}'\right)+b\left(\mathbf{q}-\mathbf{q}^h,\mathbf{q}'-\mathbf{q}^h\right) \\ &= b\left(\mathbf{q}-\mathbf{q}^h,\mathbf{q}-\mathbf{q}'\right) \\ &\leq C_2\left\|\mathbf{q}-\mathbf{q}^h\right\|_{\left(H^{-1/2}(\Gamma)\right)^2}\left\|\mathbf{q}-\mathbf{q}'\right\|_{\left(H^{-1/2}(\Gamma)\right)^2} \end{aligned} \tag{41}$$

and applying the coerciveness of $b(\cdot,\cdot)$ yields

$$b\left(\mathbf{q}-\mathbf{q}^h,\mathbf{q}-\mathbf{q}^h\right) \geq C_1\left\|\mathbf{q}-\mathbf{q}^h\right\|^2_{\left(H^{-1/2}(\Gamma)\right)^2} \tag{42}$$

thus for any $\mathbf{q}' \in \overset{\circ}{V}_h(\Gamma)$, we obtain

$$\left\|\mathbf{q}-\mathbf{q}^h\right\|_{\left(H^{-1/2}(\Gamma)\right)^2} \leq C \inf_{\mathbf{q}' \in \overset{\circ}{V}_h(\Gamma)}\left\|\mathbf{q}-\mathbf{q}'\right\|_{\left(H^{-1/2}(\Gamma)\right)^2} \tag{43}$$

Since $\mathbf{q}'$ is an arbitrary element in $\overset{\circ}{V}_h(\Gamma)$, let

$$\mathbf{q}' = S_h\mathbf{q} \tag{44}$$

where S_h denotes a projection from $L^2(\Gamma)$ onto $\overset{\circ}{V}_h(\Gamma)$. Note that $\mathbf{q}^h \neq S_h\mathbf{q}$. Hence,

$$\left\|\mathbf{q}-\mathbf{q}^h\right\|_{\left(H^{-1/2}(\Gamma)\right)^2} \leq C\left\|\mathbf{q}-S_h\mathbf{q}\right\|_{\left(H^{-1/2}(\Gamma)\right)^2} \tag{45}$$

On the other hand, from Theorem 3.1, we have

$$\left\|\mathbf{q}-S_h\mathbf{q}\right\|_{(H^0(\Gamma))^2} \leq \left\|\mathbf{q}-\mathscr{M}\mathbf{q}\right\|_{(H^0(\Gamma))^2} \leq Ch^{m+1}\left\|\mathbf{q}\right\|_{(H^{m+1}(\Gamma))^2} \tag{46}$$

thus according to a classical duality argument we deduce

$$\begin{aligned}
\|\mathbf{q}-S_h\mathbf{q}\|_{(H^{-1}(\Gamma))^2} &= \sup_{\mathbf{f}\in(H^1(\Gamma))^2} \frac{\int_\Gamma (\mathbf{q}-S_h\mathbf{q})\cdot\mathbf{f}\,\mathrm{d}S}{\|\mathbf{f}\|_{(H^1(\Gamma))^2}} \\
&= \sup_{\mathbf{f}\in(H^1(\Gamma))^2} \frac{\int_\Gamma (\mathbf{q}-S_h\mathbf{q})\cdot(\mathbf{f}-S_h\mathbf{f})\,\mathrm{d}S}{\|\mathbf{f}\|_{(H^1(\Gamma))^2}} \\
&\le \sup_{\mathbf{f}\in(H^1(\Gamma))^2} \frac{\|\mathbf{q}-S_h\mathbf{q}\|_{(H^0(\Gamma))^2}\|\mathbf{f}-S_h\mathbf{f}\|_{(H^0(\Gamma))^2}}{\|\mathbf{f}\|_{(H^1(\Gamma))^2}} \\
&\le Ch^{m+2}\|\mathbf{q}\|_{(H^{m+1}(\Gamma))^2} \qquad (47)
\end{aligned}$$

hence using an interpolation theorem of Sobolev spaces [Zhu and Yuan (2009)] leads to

$$\|\mathbf{q}-S_h\mathbf{q}\|_{\left(H^{-1/2}(\Gamma)\right)^2} \le \|\mathbf{q}-S_h\mathbf{q}\|^{1/2}_{(H^0(\Gamma))^2}\|\mathbf{q}-S_h\mathbf{q}\|^{1/2}_{(H^{-1}(\Gamma))^2} \le Ch^{m+3/2}\|\mathbf{q}\|_{(H^{m+1}(\Gamma))^2} \qquad (48)$$

Substituting Eq. (48) into Eq. (45) the proof ended.

Theorem 5.2 *Let $1/2 \le k \le \gamma+2$, then we have a constant C independent of h such that*

$$\left\|\mathbf{q}-\mathbf{q}^h\right\|_{\left(H^{-k}(\Gamma)\right)^2} \le Ch^{m+k+1}\|\mathbf{q}\|_{(H^{m+1}(\Gamma))^2}, \quad 0\le m\le\gamma \qquad (49)$$

Proof. Let $\tilde{\mathbf{q}} = (\tilde{q}_1,\tilde{q}_2) \in \left(\overset{\circ}{H}{}^{k-1}(\Gamma)\right)^2$ be the solution of

$$\tilde{g}_j(\mathbf{x}) = \sum_{i=1}^{2}\int_\Gamma U_{ij}(\mathbf{x},\mathbf{y})\,\tilde{q}_i(\mathbf{y})\,\mathrm{d}S_\mathbf{y} + \xi_j, \quad \mathbf{x}\in\Gamma \qquad (50)$$

then according to Theorem 4.1,

$$\|\tilde{\mathbf{q}}\|_{\left(H^{k-1}(\Gamma)\right)^2} \le C\|\tilde{\mathbf{g}}\|_{\left(H^k(\Gamma)/\mathbb{R}\right)^2} \qquad (51)$$

thus it follows from the classical duality argument that

$$\left\|\mathbf{q}-\mathbf{q}^h\right\|_{\left(H^{-k}(\Gamma)\right)^2} = \sup_{\tilde{\mathbf{g}}\in\left(H^k(\Gamma)/\mathbb{R}\right)^2} \frac{\left|\int_\Gamma\left(\mathbf{q}-\mathbf{q}^h\right)\cdot\tilde{\mathbf{g}}\,\mathrm{d}S\right|}{\|\tilde{\mathbf{g}}\|_{\left(H^k(\Gamma)/\mathbb{R}\right)^2}} \le C \sup_{\tilde{\mathbf{q}}\in\left(H^{k-1}(\Gamma)\right)^2} \frac{\left|b\left(\mathbf{q}-\mathbf{q}^h,\tilde{\mathbf{q}}\right)\right|}{\|\tilde{\mathbf{q}}\|_{\left(H^{k-1}(\Gamma)\right)^2}}$$

(52)

Now, we have from Eq. (40) that

$$b\left(\mathbf{q}-\mathbf{q}^h,\tilde{\mathbf{q}}\right)=b\left(\mathbf{q}-\mathbf{q}^h,\tilde{\mathbf{q}}-S_h\tilde{\mathbf{q}}\right)+b\left(\mathbf{q}-\mathbf{q}^h,S_h\tilde{\mathbf{q}}\right)=b\left(\mathbf{q}-\mathbf{q}^h,\tilde{\mathbf{q}}-S_h\tilde{\mathbf{q}}\right) \quad (53)$$

where S_h is a projection from $L^2(\Gamma)$ onto $\overset{\circ}{V}_h(\Gamma)$. Therefore, using the continuity of the bilinear form $b(\cdot,\cdot)$ and inequality (48), we have

$$\begin{aligned} b\left(\mathbf{q}-\mathbf{q}^h,\tilde{\mathbf{q}}-S_h\tilde{\mathbf{q}}\right) &\leq C\left\|\mathbf{q}-\mathbf{q}^h\right\|_{\left(H^{-1/2}(\Gamma)\right)^2}\left\|\tilde{\mathbf{q}}-S_h\tilde{\mathbf{q}}\right\|_{\left(H^{-1/2}(\Gamma)\right)^2} \\ &\leq Ch^{m+k+1}\left\|\mathbf{q}\right\|_{(H^{m+1}(\Gamma))^2}\left\|\tilde{\mathbf{q}}\right\|_{\left(H^{k-1}(\Gamma)\right)^2} \end{aligned} \quad (54)$$

The proof is completed via gathering Eqs. (52)-(54).

Remark 5.1 *Theorem 5.2 shows that the highest rate of the convergence achieved by our Galerkin method for the density function* $\mathbf{q}$ *is* $\mathrm{O}\left(h^{2\gamma+3}\right)$ *in* $H^{-\gamma-2}(\Gamma)$.

Now we are in a position to estimate an error between the solution $\mathbf{u}$ given by Eq. (17) and the approximate solution $\mathbf{u}^h$ given by Eq. (36).

Theorem 5.3 *There exists a constant C independent of h such that*

$$\left\|\mathbf{u}-\mathbf{u}^h\right\|_{(H^1(\Omega))^2\times\left(W_0^1(\Omega')\right)^2}\leq Ch^{m+3/2}\left\|\mathbf{q}\right\|_{(H^{m+1}(\Gamma))^2},\quad 0\leq m\leq\gamma \quad (55)$$

Proof. It follows immediately from Theorems 4.1 and 5.1.

Theorem 5.4 *There exists* $\delta>0$, *for* $\forall\mathbf{x}\in\mathbb{R}^2$ *with* $d(\mathbf{x},\Gamma)=\min_{\mathbf{y}\in\Gamma}\{|\mathbf{x}-\mathbf{y}|\}\geq\delta$, *we have*

$$\left|\mathbf{u}(\mathbf{x})-\mathbf{u}^h(\mathbf{x})\right|\leq C\left(\sum_{l=0}^{\gamma+2}\left(d(\mathbf{x},\Gamma)\right)^{-l}\right)h^{m+\gamma+3}\left\|\mathbf{q}\right\|_{(H^{m+1}(\Gamma))^2} \quad (56)$$

$$\left|\partial^\alpha\mathbf{u}(\mathbf{x})-\partial^\alpha\mathbf{u}^h(\mathbf{x})\right|\leq C\left(\sum_{l=0}^{\gamma+2}\left(d(\mathbf{x},\Gamma)\right)^{-l-|\alpha|}\right)h^{m+\gamma+3}\left\|\mathbf{q}\right\|_{(H^{m+1}(\Gamma))^2} \quad (57)$$

where $0\leq m\leq\gamma$, $|\alpha|=\alpha_1+\alpha_2>0$ *and C is a constant independent of h.*

Proof. According to Eqs. (17) and (36),

$$\begin{aligned} \left|u_j(\mathbf{x})-u_j^h(\mathbf{x})\right| &= \left|\sum_{i=1}^{2}\int_\Gamma U_{ij}^*(\mathbf{x},\mathbf{y})\left(q_i(\mathbf{y})-q_i^h(\mathbf{y})\right)\mathrm{d}S_\mathbf{y}\right| \\ &\le \sum_{i=1}^{2}\left\|U_{ij}^*(\mathbf{x},\mathbf{y})\right\|_{H^{\gamma+2}(\Gamma)}\left\|q_i(\mathbf{y})-q_i^h(\mathbf{y})\right\|_{H^{-\gamma-2}(\Gamma)},\ j=1,2 \quad (58) \end{aligned}$$

Because of $d(\mathbf{x},\Gamma)\ge\delta>0$, we have

$$\left\|U_{ij}^*(\mathbf{x},\mathbf{y})\right\|_{H^{\gamma+2}(\Gamma)} \le C\sum_{l=0}^{\gamma+2}\left(d(\mathbf{x},\Gamma)\right)^{-l},\quad i,j=1,2 \quad (59)$$

Thus by gathering Eqs. (49), (58) and (59) we can prove Eq. (56). The proof of Eq. (57) is similar.

Theorem 5.4 obtained the error of the displacement field $\mathbf{u}$ and its derivatives outside the neighborhood of Γ, which shows extremely high accuracy can be achieved not only for $\mathbf{u}$ but also for its derivatives. As a direct consequence, we state an error between the stress tensor σ and its approximate solution σ^h.

Corollary 5.1 *Let σ and σ^h be given by Eqs. (18) and (37), respectively. Then under conditions of Theorem 5.4, we have*

$$\left|\sigma(\mathbf{x})-\sigma^h(\mathbf{x})\right| \le C\left(\sum_{l=0}^{\gamma+2}\left(d(\mathbf{x},\Gamma)\right)^{-l-1}\right)h^{m+\gamma+3}\left\|\mathbf{q}\right\|_{(H^{m+1}(\Gamma))^2} \quad (60)$$

where $0\le m\le\gamma$ and C is a constant independent of h.

Remark 5.2 *Contrary to the case of the domain type methods, such as the FEM, Theorem 5.4 and Corollary 5.1 indicate that the errors of stress σ and displacement $\mathbf{u}$ in the GBNM are all of the same order.*

Now we examine the case inside the neighbor of Γ.

Theorem 5.5 *There exists $\delta>0$, for any $\mathbf{x}\in\mathbb{R}^2$ with $d(\mathbf{x},\Gamma)<\delta$ and for given $\varepsilon>0$, we have a constant C independent of h such that*

$$\left|\mathbf{u}(\mathbf{x})-\mathbf{u}^h(\mathbf{x})\right| \le C(\delta)\,h^{m+1-\varepsilon}\left\|\mathbf{q}\right\|_{(H^{m+1}(\Gamma))^2},\quad \varepsilon\le m\le\gamma \quad (61)$$

Proof. We have

$$\left|u_j(\mathbf{x})-u_j^h(\mathbf{x})\right| \leq \sum_{i=1}^{2} \left\|U_{ij}(\mathbf{x},\mathbf{y})\right\|_{H^{-\varepsilon}(\Gamma)} \left\|q_i(\mathbf{y})-q_i^h(\mathbf{y})\right\|_{H^{\varepsilon}(\Gamma)} \tag{62}$$

Let $k=\frac{2}{1+\varepsilon}$, then $0<k<2$. Thus according to the Sobolev imbedding theorem, $L^2(\Gamma)\hookrightarrow L^k(\Gamma)\hookrightarrow H^{-\varepsilon}(\Gamma)$. As a result,

$$\left\|U_{ij}(\mathbf{x},\mathbf{y})\right\|_{H^{-\varepsilon}(\Gamma)} \leq C\left\|\ln|\mathbf{x}-\mathbf{y}|\right\|_{H^{-\varepsilon}(\Gamma)} \leq C\left\|\ln|\mathbf{x}-\mathbf{y}|\right\|_{L^2(\Gamma)} \tag{63}$$

Let $\Gamma^*=\{\mathbf{y}\in\Gamma:|\mathbf{x}-\mathbf{y}|<\delta\}$ and $\ell_{\mathbf{x}}=\max_{\mathbf{y}\in\Gamma}\{|\mathbf{x}-\mathbf{y}|\}$, then

$$\begin{aligned}
\left\|\ln|\mathbf{x}-\mathbf{y}|\right\|_{L^2(\Gamma)}^2 &= \int_{\Gamma/\Gamma^*}\left|\ln|\mathbf{x}-\mathbf{y}|\right|^2 \mathrm{d}S_{\mathbf{x}} + \int_{\Gamma^*}\left|\ln|\mathbf{x}-\mathbf{y}|\right|^2 \mathrm{d}S_{\mathbf{x}} \\
&\leq \int_{\Gamma/\Gamma^*}\left(\max\{|\ln\ell_{\mathbf{x}}|,|\ln\delta|\}\right)^2 \mathrm{d}S_{\mathbf{y}} + \delta|\ln\delta|^2 + 2\delta|\ln\delta| + 2\int_{\Gamma^*}\mathrm{d}S_{\mathbf{y}} \\
&\leq \mathrm{mes}(\Gamma)\left(\max\{|\ln\ell_{\mathbf{y}}|,|\ln\delta|\}^2\right) + \delta|\ln\delta|^2 + 2\delta|\ln\delta| + 2\mathrm{mes}(\Gamma)
\end{aligned} \tag{64}$$

so

$$\left\|U_{ij}(\mathbf{x},\mathbf{y})\right\|_{H^{-\varepsilon}(\Gamma)} \leq C(\delta) \tag{65}$$

Besides, using the triangle inequality yields

$$\left\|\mathbf{q}-\mathbf{q}^h\right\|_{(H^{\varepsilon}(\Gamma))^2} \leq \left\|\mathbf{q}-S_h\mathbf{q}\right\|_{(H^{\varepsilon}(\Gamma))^2} + \left\|S_h\mathbf{q}-\mathbf{q}^h\right\|_{(H^{\varepsilon}(\Gamma))^2} \tag{66}$$

On the one hand, according to Lemma 5.1, Theorem 3.1 and Eq. (46) we have

$$\begin{aligned}
\left\|\mathbf{q}-S_h\mathbf{q}\right\|_{(H^{\varepsilon}(\Gamma))^2} &\leq \left\|\mathbf{q}-\mathscr{M}\mathbf{q}\right\|_{(H^{\varepsilon}(\Gamma))^2} + \left\|\mathscr{M}\mathbf{q}-S_h\mathbf{q}\right\|_{(H^{\varepsilon}(\Gamma))^2} \\
&\leq \left\|\mathbf{q}-\mathscr{M}\mathbf{q}\right\|_{(H^{\varepsilon}(\Gamma))^2} + Ch^{-\varepsilon}\left\|\mathscr{M}\mathbf{q}-S_h\mathbf{q}\right\|_{(H^{0}(\Gamma))^2} \\
&\leq \left\|\mathbf{q}-\mathscr{M}\mathbf{q}\right\|_{(H^{\varepsilon}(\Gamma))^2} + Ch^{-\varepsilon}\left\{\left\|\mathscr{M}\mathbf{q}-\mathbf{q}\right\|_{(H^{0}(\Gamma))^2}\right. \\
&\quad \left. + \left\|\mathbf{q}-S_h\mathbf{q}\right\|_{(H^{0}(\Gamma))^2}\right\} \\
&\leq Ch^{m+1-\varepsilon}\left\|\mathbf{q}\right\|_{(H^{m+1}(\Gamma))^2}, \quad \varepsilon\leq m\leq\gamma
\end{aligned} \tag{67}$$

and, on the other hand, from Lemma 5.1, Theorem 5.1 and Eq. (48) we also have

$$\begin{aligned}
\left\|S_h\mathbf{q}-\mathbf{q}^h\right\|_{(H^{\varepsilon}(\Gamma))^2} &\leq Ch^{-1/2-\varepsilon}\left\|S_h\mathbf{q}-\mathbf{q}^h\right\|_{\left(H^{-1/2}(\Gamma)\right)^2} \\
&\leq Ch^{-1/2-\varepsilon}\left(\left\|S_h\mathbf{q}-\mathbf{q}\right\|_{\left(H^{-1/2}(\Gamma)\right)^2} + \left\|\mathbf{q}-\mathbf{q}^h\right\|_{\left(H^{-1/2}(\Gamma)\right)^2}\right) \\
&\leq Ch^{m+1-\varepsilon}\left\|\mathbf{q}\right\|_{(H^{m+1}(\Gamma))^2}, \quad \varepsilon\leq m\leq\gamma
\end{aligned} \tag{68}$$

Thus,

$$\left\|\mathbf{q}-\mathbf{q}^h\right\|_{(H^\varepsilon(\Gamma))^2} \leq Ch^{m+1-\varepsilon}\left\|\mathbf{q}\right\|_{(H^{m+1}(\Gamma))^2}, \quad \varepsilon \leq m \leq \gamma \tag{69}$$

Finally, the theorem follows by collecting Eqs. (62), (65) and (69).

Remark 5.3 *Because* $\partial\mathbf{u}/\partial\mathbf{n}$ *is discontinuous at the points of* Γ*, we cannot obtain error of* $|\partial\mathbf{u}-\partial\mathbf{u}_h|$ *inside the neighborhood of* Γ.

6 Numerical experiments

In the following test examples we restrict ourselves to elastic problems whose analytic are available and, therefore, our numerical solutions can easily be compared. Here we used uniformly distributed boundary nodes. Besides, the polynomial basis is chosen as a quadratic basis, and the weight function is a cubic spline function

$$w_i(\mathbf{x}) = \begin{cases} 2/3-4d^2+4d^3, & d \leq 1/2 \\ 4/3-4d+4d^2-4d^3/3, & 1/2 < d \leq 1 \\ 0, & d > 1 \end{cases} \tag{70}$$

where $d = |\mathbf{x}-\mathbf{x}_i|/h$, h is the radius of the weight functions. In all examples, h is taken to be $3.0\bar{d}$, with $\bar{d}$ as the nodal spacing.

6.1 Patch test

Consider the standard patch test in a square of dimensional 1×1. The origin of the coordinate is located on the left lower corner of the patch. This is a Dirichlet problem for the displacements [Kothnur, Mukherjee, and Mukherjee (1999)]

$$u_1 = 2x_1+3x_2, \quad u_2 = 3x_1+2x_2 \tag{71}$$

The comparison of the exact solutions and numerical solutions with 40 nodes are plotted in Fig. 1. It is clearly shown that the numerical solutions are in excellent agreement with the exact solutions. Thus we can conclude that the proposed method can pass the patch test successfully.

Besides, Tab. 1 shows the comparison of the displacements obtained by the GBNM and the BNM [Kothnur, Mukherjee, and Mukherjee (1999)] at various points. It can be found that the GBNM results are more accurate than the BNM results.

6.2 Cantilever beam

The second example involves the well-known cantilever beam which is shown in Fig. 2. The length and width of the beam are $L = 48$m and $D = 12$m, respectively.

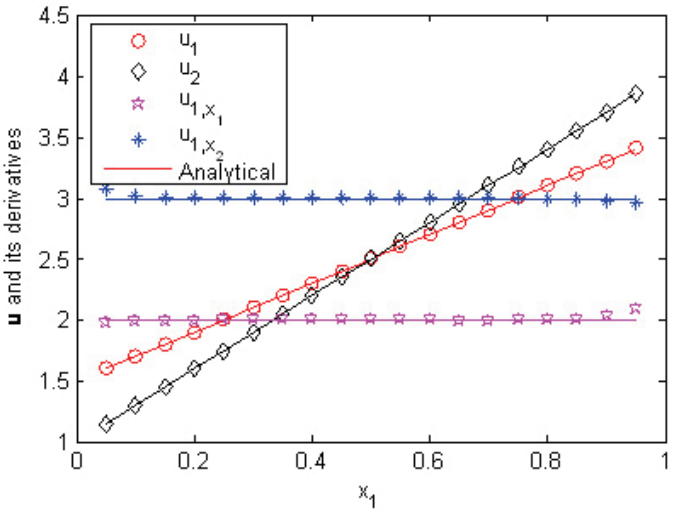

Figure 1: Displacement **u** and its derivatives at $x_2 = 0.5$ for the patch test

Table 1: Relative errors at various points for the patch test ($N = 80$)

Location	Error in $[u_1]$%		Error in $[u_2]$%	
	GBNM	BNM	GBNM	BNM
0.25, 0.25	0.004	0.336	0.004	0.336
0.25, 0.50	-0.001	0.180	0.000	0.051
0.25, 0.75	-0.002	0.116	0.000	-0.014
0.50, 0.25	0.000	0.051	-0.001	0.180
0.50, 0.50	-0.003	0.000	-0.003	0.000
0.50, 0.75	-0.004	-0.096	-0.003	-0.011
0.75, 0.25	0.000	-0.014	-0.002	-0.012
0.75, 0.50	-0.003	-0.012	-0.004	-0.027
0.75, 0.75	-0.007	-0.011	-0.007	-0.011

The load is $P = 1000$kN. A plain stress condition is considered. The other parameters that are used in our analysis are Young's modulus $E = 3.0 \times 10^7$kPa and Poisson's ration $\nu = 0.3$. The analytical solution is given by

$$u_1 = \frac{Px_2}{6EI}\left[(6L - 3x_1)x_1 + (2+\nu)\left(x_2^2 - \frac{D^2}{4}\right)\right] \tag{72}$$

$$u_2 = -\frac{P}{6EI}\left[3\nu x_2^2(L-x_1)+(4+5\nu)\frac{D^2 x_1}{4}+(3L-x_1)x_1^2\right] \tag{73}$$

where the moment of inertia I of the beam is given by $I = D^3/12$.
The stresses corresponding to the displacements are

$$\sigma_{11} = \frac{P(L-x_1)x_2}{I}, \quad \sigma_{22} = 0, \quad \sigma_{12} = -\frac{P}{2I}\left(\frac{D^2}{4}-x_2^2\right) \tag{74}$$

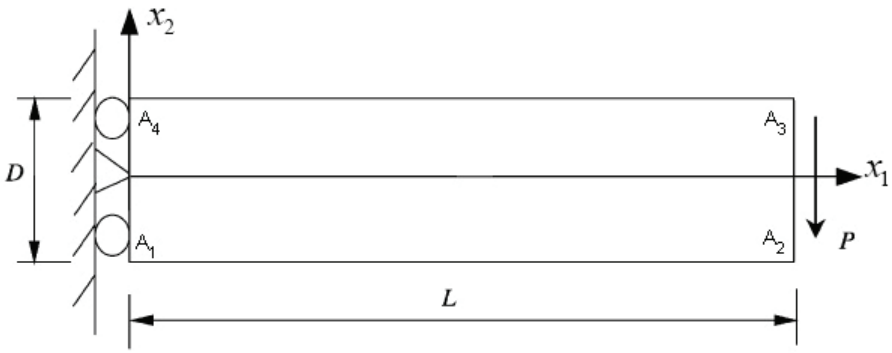

Figure 2: A cantilever beam with a parabolic traction at the free end

Fig. 3 and Fig. 4 display a comparison between the present numerical results with the exact solutions for displacement $\mathbf{u}$ and stress σ, respectively. In this analysis, we applied 80 boundary nodes. Excellent agreement between the solutions is achieved in both figures.

To show the convergence of the presented method, regularly distributed 20, 40, 80 and 160 nodes are used. In this study, the ratio of the number of nodes on A_1A_2 and A_3A_4 to that on A_1A_4 and A_2A_3 is kept constant and equal to 4. The results of convergence of $\mathbf{u}$ are shown in Fig. 5. It is observed that the numerical rate matches our theoretical result.

For investigating the behavior of points far away from the boundary and near the boundary, the values of the numerical approximations of displacement $\mathbf{u}$ and stress σ at some inner points are given in Tab. 2. The results show that the error decreases with the increase of the boundary nodes. The numerical convergence rates of $\mathbf{u}$ and σ match our theoretical results for points far away from the boundary. While points lie in the neighborhood of Γ, the numerical results of $\mathbf{u}$ also confirm the theoretical error statements.

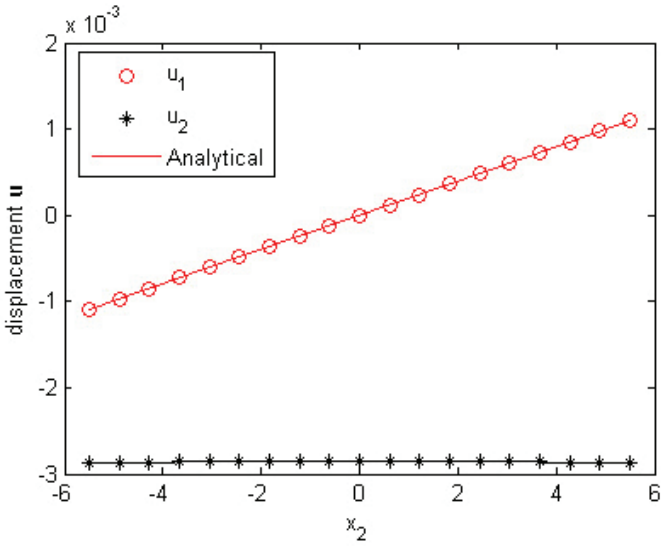

Figure 3: Results of displacement $\mathbf{u}$ for cantilever beam at the section $x_1 = \frac{L}{2}$

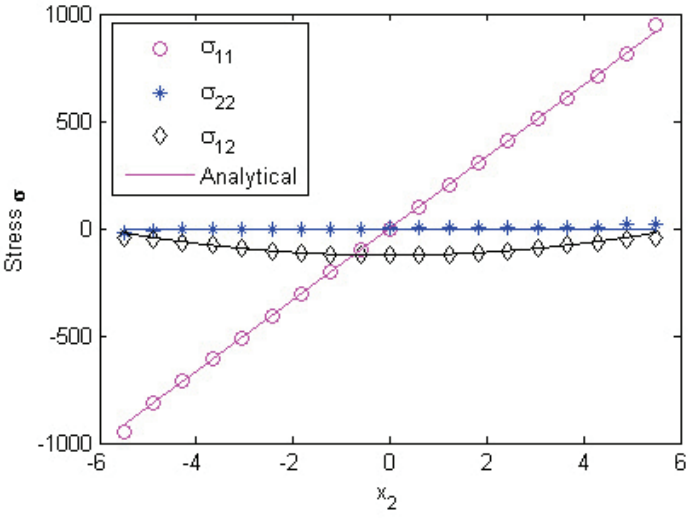

Figure 4: Stress σ along the line $x_1 = \frac{L}{2}$ for the cantilever beam

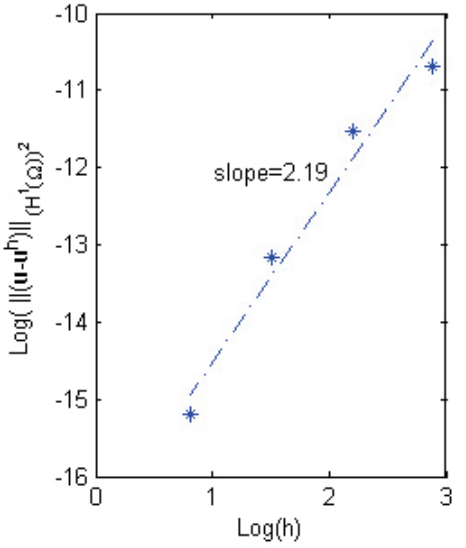

Figure 5: The convergence for the cantilever problem

Table 2: Approximations and convergence rates for the cantilever beam

x_1, x_2		Numerical solutions				Exact	Rates
		N=20	N=40	N=80	N=160		
30.0, 0.00	$u_1(*10^{-7})$	-0.28745	0.05436	-0.00270	0.00040	0.00000	3.28
	$u_2(*10^{-2})$	-0.41851	-0.41896	-0.41875	-0.41875	-0.41875	3.32
	σ_{11}	0.99897	-0.15223	-0.00230	0.00026	0.00000	4.18
	σ_{22}	-0.71990	0.27087	0.00170	0.00002	0.00000	5.25
	$\sigma_{12}(*10^{2})$	-0.79391	-1.32595	-1.24983	-1.24991	-1.25000	4.55
12.0, 1.20	$u_1(*10^{-3})$	0.13400	0.13682	0.13632	0.13632	0.13632	4.58
	$u_2(*10^{-2})$	-0.08112	-0.08304	-0.08267	-0.08268	-0.08268	3.40
	$\sigma_{11}(*10^{2})$	3.10274	3.08926	3.00069	3.00009	3.00000	3.75
	$\sigma_{22}(*10^{1})$	4.07492	-2.08392	-0.01153	-0.00117	0.00000	4.28
	$\sigma_{12}(*10^{2})$	-1.61741	-1.06580	-1.20098	-1.20017	-1.20000	4.08
30.0, 5.0000	$u_1(*10^{-2})$	0.11262	0.11432	0.11407	0.11410	0.11410	3.07
30.0, 5.9000	$u_1(*10^{-2})$	0.13355	0.13566	0.13504	0.13515	0.13515	2.52
30.0, 5.9900	$u_1(*10^{-2})$	0.13500	0.13741	0.13699	0.13726	0.13726	2.57
30.0, 5.9990	$u_1(*10^{-2})$	0.13512	0.13754	0.13713	0.13741	0.13748	1.27
30.0, 5.9999	$u_1(*10^{-2})$	0.13513	0.13755	0.13714	0.13742	0.13750	1.20

6.3 Exterior problems

The following displacement field, which is an exact solution of the elasticity Navier equations of problem (11), is imposed at the displacement nodes on the boundary:

$$u_1 = \frac{x_1}{x_1^2+x_2^2}, \quad u_2 = \frac{x_2}{x_1^2+x_2^2}, \quad \text{in } \Omega' = \mathbb{R}^2/([-1,1]\times[-1,1]) \tag{75}$$

This exterior problem is solved for the plane strain case with the Poisson's ration $\nu = 0.3$ and Young's modulus $E = 2.5$. The numerical results are compared against analytical solutions as shown in Fig. 6 and Fig. 7. In this analysis, we employed 32 boundary nodes. The numerical solutions are seen to capture the behavior of the exact solutions very well.

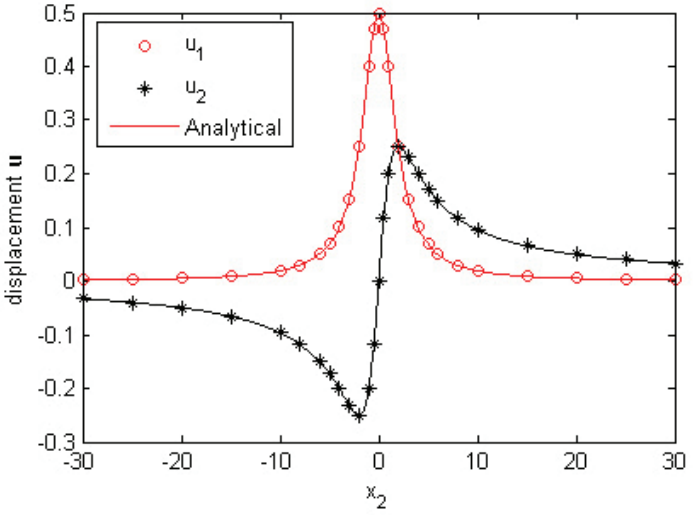

Figure 6: Displacement **u** for the exterior problem along the line $x_1 = 2$

When four different regular nodes arrangements of 2, 4, 8 and 16 nodes on each edge have been used, the convergence rate is plotted with respect to Sobolev norms in Fig. 8. Here again, the convergence is in accordance with our theoretical result.

The values of the numerical solutions of **u** and σ at some inner points are displayed in Tab. 3. As we expected, the results from the proposed meshless method gradually converge to the exact values along with the decrease of the radii of the weight functions, and the numerical results also confirm theoretical results.

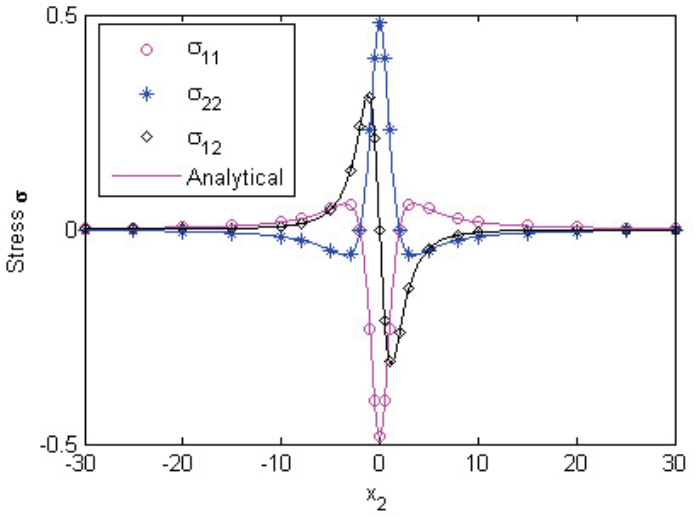

Figure 7: Stress components for the exterior problem along $x_1 = 2$

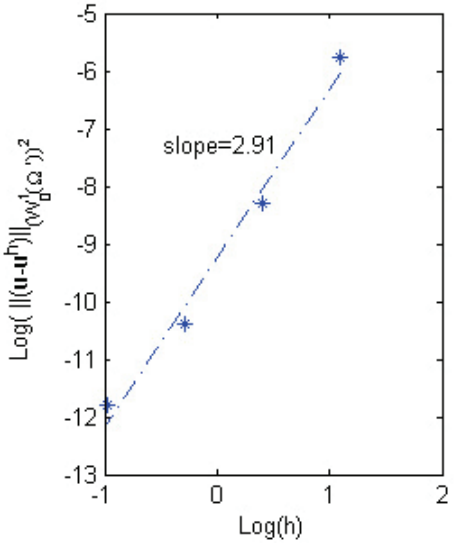

Figure 8: Convergence of the exterior problem

7 Conclusions

The Galerkin boundary node method (GBNM) based on a variational formulation of BIEs and the MLS technique is developed in this paper for linear elasticity. Com-

Table 3: Approximations and convergence rates for the exterior problem

x_1, x_2		Numerical solutions				Exact	Rates
		N=8	N=16	N=32	N=64		
10.0, 10.0	$u_1(*10^{-1})$	0.59006	0.54211	0.50013	0.50006	0.50000	4.01
	$u_2(*10^{-1})$	0.01625	0.49683	0.50023	0.50004	0.50000	4.47
	$\sigma_{11}(*10^{-3})$	-0.48694	0.13116	0.00067	-0.00023	0.00000	4.08
	$\sigma_{22}(*10^{-2})$	-0.15504	0.00608	-0.00011	0.00001	0.00000	4.61
	$\sigma_{12}(*10^{-2})$	-1.11253	-0.94890	-0.96191	-0.96164	-0.96154	3.69
0.2, 1.1000	u_2	0.83392	0.88297	0.88010	0.87995	0.88000	3.41
0.2, 1.0100	u_2	0.82090	0.94168	0.93179	0.95181	0.95274	2.05
0.2, 1.0010	u_2	0.81914	0.93864	0.93041	0.95444	0.96065	1.31
0.2, 1.0001	u_2	0.81898	0.93835	0.93030	0.95457	0.96145	1.27

pared with domain type meshless method, such as the EFGM, the LBIE method and the MLPG approach, the new approach is a boundary type meshless method which has the well-known dimensionality of the BEM; compared with the conventional BEM, it is a meshless method which requires only a nodal data structure on the bounding surface of the domain to be solved; compared with other meshless methods such as the BNM and the EFGM where introducing the MLS also, boundary conditions in the GBNM can be satisfied easily and directly in terms of multiplying the boundary function by a test function and integrating over the boundary.

We set up a framework for error estimates of the GBNM in Sobolev spaces. The error results show that the error bound of the numerical solution is directly related to the radii of the weight functions. Besides, the displacement field and the stress field possess L^∞-superconvergence outside the neighborhood of Γ, they hold the same convergence rate. Furthermore, we have got the convergence of the displacement in L^∞ norm in the vicinity of Γ. Some numerical tests have been given and the numerical results are accurate and are in agreement with the theoretical analysis.

In the GBNM, the symmetry and positive definiteness of the variational problems can be kept. The property of symmetry can be an added advantage in coupling the GBNM with the FEM or other established meshless methods. This coupled technique is especially suited for the problems with unbounded domain. This is a subject of the further studies.

References

Arefmanesh, A.; Najafi, M.; Abdi, H. (2008): Meshless local Petrov-Galerkin method with unity test function for non-isothermal fluid flow. *CMES: Computer Modeling in Engineering & Sciences*, vol. 25, pp. 9–22.

Atluri, S. N.; Liu, H. T.; Han, Z. D. (2006): Meshless local Petrov-Galerkin (MLPG) mixed collocation method for elasticity problems. *CMES: Computer Modeling in Engineering & Sciences*, vol. 14, pp. 141–152.

Atluri, S. N.; Shen, S. P. (2002): The meshless local Petrov-Galerkin (MLPG) method: a simple & less-costly alternative to the finite element and boundary element methods. *CMES: Computer Modeling in Engineering & Sciences*, vol. 3, pp. 11–51.

Atluri, S. N.; Sladek, J.; Sladek, V.; Zhu, T. (2000): The local boundary integral equation (LBIE) and it's meshless implementation for linear elasticity. *Computational Mechanics*, vol. 25, pp. 180–198.

Belytschko, T.; Krongauz, Y.; Organ, D.; Fleming, M. (1996): Meshless methods: an overview and recent developments. *Computer Methods in Applied Mechanics and Engineering*, vol. 139, pp. 3–47.

Brezzi, F. (1974): On the existence, uniqueness and approximation of saddle-point problems arising from Lagrange multipliers. *RAIRO Analyse Numérique*, vol. R2, pp. 129–151.

Chen, W. H.; Chi, C. T.; Lee, M. H. (2009): A novel element-free Galerkin method with uniform background grid for extremely deformed problems. *CMES: Computer Modeling in Engineering & Sciences*, vol. 40, pp. 175–200.

Dautray, R.; Lious, J. L. (2000): *Mathematical Analysis and Numerical Methods for Science and Technology. Volume 4: Integral Equations and Numerical Methods*. Springer, Berlin.

Duarte, C. A.; Oden, J. T. (1996): H-p clouds—an h-p meshless method. *Numerical Methods for Partial Differential Equations*, vol. 12, pp. 675–705.

Gu, Y. T.; Liu, G. R. (2002): A boundary point interpolation method for stress analysis of solids. *Computational Mechanics*, vol. 28, pp. 47–54.

Hagihara, S.; Tsunori, M.; Ikeda, T.; Miyazaki, N. (2007): Application of meshfree method to elastic-plastic fracture mechanics parameter analysis. *CMES: Computer Modeling in Engineering & Sciences*, vol. 17, pp. 63–72.

Han, Z. D.; Atluri, S. N. (2004): Meshless local Petrov-Galerkin (MLPG) approaches for solving 3D problems in elasto-statics. *CMES: Computer Modeling in Engineering & Sciences*, vol. 6, pp. 169–188.

Haq, S.; Islam, S.; Ali, A. (2008): A numerical meshfree technique for the solution of the MEW equation. *CMES: Computer Modeling in Engineering & Sciences*, vol. 38, pp. 1–24.

Haq, S.; Islam, S.; Uddin, M. (2009): Numerical solution of nonlinear schrodinger equations by collocation method using radial basis functions. *CMES: Computer Modeling in Engineering & Sciences*, vol. 44, pp. 115–135.

Ho-Minh, D.; Mai-Duy, N.; Tran-Cong, T. (2009): A Galerkin-RBF approach for the streamfunction-vorticity-temperature formulation of natural convection in 2D enclosured domains. *CMES: Computer Modeling in Engineering & Sciences*, vol. 44, pp. 219–248.

Hsiao, G. C.; Wendland, W. L. (2008): *Boundary integral equations*. Springer, Berlin.

Johnson, J. N.; Owen, J. M. (2007): A meshless local Petrov-Galerkin method for magnetic diffusion in non-magnetic conductors. *CMES: Computer Modeling in Engineering & Sciences*, vol. 22, pp. 165–188.

Kosec, G.; Sarler, B. (2008): Local RBF collocation method for Darcy flow. *CMES: Computer Modeling in Engineering & Sciences*, vol. 25, pp. 197–207.

Kothnur, V. S.; Mukherjee, S.; Mukherjee, Y. X. (1999): Two-dimensional linear elasticity by the boundary node method. *International Journal of Solids and Structures*, vol. 36, pp. 1129–1147.

Li, L.; Liu, S.; Wang, H. (2008): Meshless analysis of ductile failure. *CMES: Computer Modeling in Engineering & Sciences*, vol. 36, pp. 173–192.

Li, X.; Zhu, J. (2009): A Galerkin boundary node method and its convergence analysis. *Journal of Computational and Applied Mathematics*, vol. 230, pp. 314–328.

Li, X.; Zhu, J. (2009): A Galerkin boundary node method for biharmonic problems. *Engineering Analysis with Boundary Elements*, vol. 33, pp. 858–865.

Libre, N. A.; Emdadi, A.; Kansa, E. J.; Rahimian, M.; Shekarchi, M. (2008): A stabilized RBF collocation scheme for Neumann type boundary value problems. *CMES: Computer Modeling in Engineering & Sciences*, vol. 24, pp. 61–80.

Liu, G. R.; Gu, Y. T. (2004): Boundary meshfree methods based on the boundary point interpolation methods. *Engineering Analysis with Boundary Elements*, vol. 28, pp. 475–487.

Liu, Y. H.; Chen, S. S.; Li, J.; Cen, Z. Z. (2008): A meshless local natural neighbour interpolation method applied to structural dynamic analysis. *CMES: Computer Modeling in Engineering & Sciences*, vol. 31, pp. 145–156.

Long, S. Y.; Liu, K. Y.; Li, G. Y. (2008): An analysis for the elasto-plastic fracture problem by the meshless local Petrov-Galerkin method. *CMES: Computer Modeling in Engineering & Sciences*, vol. 28, pp. 203–216.

Ma, Q. W. (2007): Numerical generation of freak waves using MLPG-R and QALE-FEM methods. *CMES: Computer Modeling in Engineering & Sciences*, vol. 18, pp. 223–234.

Ma, Q. W.; Zhou, J. T. (2009): MLPG-R method for numerical simulation of 2D breaking waves. *CMES: Computer Modeling in Engineering & Sciences*, vol. 43, pp. 277–303.

Mai-Cao, L.; Tran-Cong, T. (2008): A meshless approach to capturing moving interfaces in passive transport problems. *CMES: Computer Modeling in Engineering & Sciences*, vol. 31, pp. 157–188.

Mai-Duy, N.; Mai-Cao, L.; Tran-Cong, T. (2007): Computation of transient viscous flows using indirect radial basis function networks. *CMES: Computer Modeling in Engineering & Sciences*, vol. 18, pp. 59–78.

Mohammadi, M. H. (2008): Stabilized meshless local Petrov-Galerkin (MLPG) method for incompressible viscous fluid flows. *CMES: Computer Modeling in Engineering & Sciences*, vol. 29, pp. 75–94.

Moulinec, C.; Issa, R.; Marongiu, J. C.; Violeau, D. (2008): Parallel 3-D SPH simulations. *CMES: Computer Modeling in Engineering & Sciences*, vol. 25, pp. 133–147.

Mukherjee, Y. X.; Mukherjee, S. (1997): The boundary node method for potential problems. *International Journal for Numerical Methods in Engineering*, vol. 40, pp. 797–815.

Namdeo, V.; Manohar, C. S. (2008): Force state maps using reproducing kernel particle method and kriging based functional representations. *CMES: Computer Modeling in Engineering & Sciences*, vol. 32, pp. 123–159.

Pini, G.; Mazzia, A.; Sartoretto, F. (2008): Accurate MLPG solution of 3D potential problems. *CMES: Computer Modeling in Engineering & Sciences*, vol. 36, pp. 43–64.

Sageresan, N.; Drathi, R. (2008): Crack propagation in concrete using meshless method. *CMES: Computer Modeling in Engineering & Sciences*, vol. 32, pp. 103–112.

Sellountos, E. J.; Sequeira1, A.; Polyzos, D. (2009): Elastic transient analysis with MLPG (LBIE) method and local RBFs. *CMES: Computer Modeling in Engineering & Sciences*, vol. 41, pp. 215–241.

Shaw, A.; Roy, D. (2007): A novel form of reproducing kernel interpolation method with applications to nonlinear mechanics. *CMES: Computer Modeling in Engineering & Sciences*, vol. 19, pp. 69–98.

Shim, H.; Ho, V. T. T.; Wang, S.; Tortorelli, D. A. (2008): Topological shape optimization of electromagnetic problems using level set method and radial basis function. *CMES: Computer Modeling in Engineering & Sciences*, vol. 37, pp. 175–202.

Sladek, J.; Sladek, V.; Solek, P. (2009): Elastic analysis in 3D anisotropic functionally graded solids by the MLPG. *CMES: Computer Modeling in Engineering & Sciences*, vol. 43, pp. 223–251.

Sladek, J.; Sladek, V.; Solek, P.; Wen, P. H. (2008): Thermal bending of Reissner-Mindlin plates by the MLPG. *CMES: Computer Modeling in Engineering & Sciences*, vol. 28, pp. 57–76.

Sladek, J.; Sladek, V.; Solek, P.; Wen, P. H.; Atluri, S. N. (2008): Thermal analysis of Reissner-Mindlin shallow shells with FGM properties by the MLPG. *CMES: Computer Modeling in Engineering & Sciences*, vol. 30, pp. 77–98.

Sladek, J.; Sladek, V.; Tan, C.; Atluri, S. N. (2008): Analysis of transient heat conduction in 3D anisotropic functionally graded solids by the MLPG method. *CMES: Computer Modeling in Engineering & Sciences*, vol. 32, pp. 161–174.

Sladek, J.; Sladek, V.; Zhang, C.; Solek, P. (2007): Application of the MLPG to thermo-piezoelectricity. *CMES: Computer Modeling in Engineering & Sciences*, vol. 22, pp. 217–233.

Wen, P. H.; Aliabadi, M. H.; Liu, Y. W. (2008): Meshless method for crack analysis in functionally graded materials with enriched radial base functions. *CMES: Computer Modeling in Engineering & Sciences*, vol. 30, pp. 133–147.

Wen, P. H.; Hon, Y. C. (2007): Geometrically nonlinear analysis of Reissner-Mindlin plate by meshless computation. *CMES: Computer Modeling in Engineering & Sciences*, vol. 21, pp. 177–191.

Wong, S.; Shie, Y. (2008): Large deformation analysis with Galerkin based smoothed particle hydrodynamics. *CMES: Computer Modeling in Engineering & Sciences*, vol. 36, pp. 97–118.

Wu, C. P.; Chiu, K. H.; Wang, Y. M. (2008): A differential reproducing kernel particle method for the analysis of multilayered elastic and piezoelectric plates. *CMES: Computer Modeling in Engineering & Sciences*, vol. 27, pp. 163–186.

Wu, X. H.; Shen, S. S.; Tao, T. W. (2007): Meshless local Petrov-Galerkin collocation method for two-dimensional heat conduction problems. *CMES: Computer Modeling in Engineering & Sciences*, vol. 22, pp. 65–76.

Zhang, Y. Y.; Chen, L. (2008): A simplified meshless method for dynamic crack growth. *CMES: Computer Modeling in Engineering & Sciences*, vol. 31, pp. 189–199.

Zhao, M.; Nie, Y. (2008): A study of boundary conditions in the meshless local Petrov-Galerkin (MLPG) method for electromagnetic field computations. *CMES: Computer Modeling in Engineering & Sciences*, vol. 37, pp. 97–112.

Zheng, J.; Long, S.; Xiong, Y.; Li, G. (2009): A finite volume meshless local Petrov-Galerkin method for topology optimization design of the continuum structures. *CMES: Computer Modeling in Engineering & Sciences*, vol. 42, pp. 19–34.

Zhu, J.; Yuan, Z. (2009): *Boundary element analysis*. Science Press, Beijing.